Original Paper

Cellular Physiology and Biochemistry

Cell Physiol Biochem 2010;25:91-102

Accepted: July 26, 2009

2-APB and Capsazepine-induced Ca^{2+} Influx Stimulates Clathrin-dependent Endocytosis in Alveolar Epithelial Cells

Shariq M. Usmani[1], Giorgio Fois[1], Susanne Albrecht[1], Sonja von Aulock[2], Paul Dietl[1] and Oliver H. Wittekindt[1]

[1]Institute of General Physiology, University of Ulm, Ulm [2]Biochemical Pharmacology and Zukunftskolleg, University of Konstanz, Konstanz

Key Words

Alveolar type II cells • NCI-H441 cells • 2-APB • Capsazepine • Ca^{2+} • Endocytosis

Abstract

Calcium as a second messenger influences many cellular and physiological processes. In lung, alveolar type II (ATII) cells sense mechanical stress and respond by Ca^{2+} dependent release of surfactant, which is essential for respiratory function. Nevertheless, Ca^{2+} signaling mechanisms in these cells - in particular Ca^{2+} entry pathways are still poorly understood. Herein, we investigated pharmacological properties of non-voltage-gated Ca^{2+} channel modulators in ATII and NCI-H441 cells and demonstrate that 2-Aminoethoxydiphenyl-borinate (2-APB) and capsazepine (CPZ) activate Ca^{2+} entry with pharmacologically distinguishable components. Surprisingly, 2-APB and CPZ activated clathrin dependent endocytosis in ATII and NCI-H441 cells, which was dependent on Ca^{2+} entry. The internalized material accumulated in non-acidic granules distinct from surfactant containing lamellar bodies (LB). LB exocytosis was not observed under these conditions. Our study demonstrates that 2-APB/CPZ induces Ca^{2+} entry which unlike ATP- or stretch-induced Ca^{2+} entry in ATII cells does not activate exocytosis but an opposing endocytotic mechanism.

Introduction

Calcium signaling in distal airway epithelial cells is associated with cellular response to mechanical stress or purinergic agonists such as ATP [1-3]. In alveolar type II (ATII) cells tensile strain causes the release of surfactant via elevation of the cytoplasmic Ca^{2+} concentration ($[Ca^{2+}]_c$) [2]. Both, the duration and the intensity of $[Ca^{2+}]_c$ determines the probability of surfactant storing vesicles (lamellar bodies, LB) to fuse with the plasma membrane and to release surfactant via exocytosis [3].

The mechanically induced Ca^{2+} signaling in ATII cells is considered to depend on the one hand on Ca^{2+} release from intra-cellular stores but also on Ca^{2+} entry via mechano-sensitive cation channels or, at least partly, also on store operated Ca^{2+} (SOC) entry pathways [2]. The latter may also play an important role for sustained cellular response to ATP. Ca^{2+} conducting ion channels of the transient receptor potential (TRP) channel superfamily as well as SOC channels might be possible candidates to mediate this complex Ca^{2+} signaling in ATII cells. Ion

KARGER

Fax +41 61 306 12 34
E-Mail karger@karger.ch
www.karger.com

1015-8987/10/0251-0091$26.00/0

Accessible online at:
www.karger.com/cpb

Dr. Oliver H. Wittekindt
Institute of General Physiology, University of Ulm
Albert-Einstein-Allee 11, 89081 Ulm (Germany)
Tel. +49 731 50023247, Fax +49 731 50023242
E-Mail oliver.wittekindt@uni-ulm.de

channels of the transient receptor potential (TRP) family are commonly discussed as mechanically activated ion channels [4]. Furthermore, TRP channels of the vanilloid receptor subfamily were demonstrated to mediate mechanically induced Ca^{2+} entry in airway epithelial cells [5].

SOC entry may play a role under various types of stimulation including mechanical stress [2]. SOC channels consist of the regulatory subunits STIM1 and STIM2 [6] and their interacting pore forming protein partners Orai1, -2 and -3 [6-9]. They form either homomeric or heteromeric protein complexes with distinct biophysical and pharmacological properties [10]. However, TRP subunits are also considered to be involved in SOC entry. Members of canonical TRP channels, TRPC channels are suggested to be part of SOC channels or at least are involved in regulating SOC dependent Ca^{2+} entry [11-14]. The contribution of TRP channels as part of the SOC machinery became even more evident when the formation of ternary complexes of TRPC1, Orai1 and STIM1 was shown to be relevant for SOC channel function [15].

Even though the release of surfactant is absolutely essential for lung function and its regulatory mechanisms are of certain clinical and patho-physiological interest, the characterization of Ca^{2+} entry pathways which regulate surfactant secretion and other Ca^{2+} regulated processes in these cells are sparse and poorly understood. Therefore, the pharmacological and functional characterisation of Ca^{2+} signaling pathways in ATII cells is of great interest. To aim at the identification of possible Ca^{2+} conducting ion channels which mediate Ca^{2+} signaling in ATII cells, we investigated Ca^{2+} signaling pathways in primary cultivated ATII and NCI-H441 cells, models for distal airway epithelial cells [16, 17]. In these cells 2-APB as well as the TRP-V1 inhibitor capsazepine (CPZ) induced a complex Ca^{2+} influx pathway that could be inhibited by known blockers of TRP/SOC channels. This Ca^{2+} entry induces massive clathrin mediated endocytosis, which is contrary to elevations of $[Ca^{2+}]_c$ by a multitude of other stimuli that cause LB exocytosis [2, 3, 18].

Materials and Methods

Materials

RPMI 1640 medium (PAN Biotech GmbH), fetal bovine serum (Perbio, Bonn Germany), sodium pyruvate (PAA cell culture company, Cölbe, Germany), penicillin (100 units/ml) and streptomycin (100 µg/ml) (Invitrogen, Karlsruhe, Germany), Brilliant Black (BB) (MP Biomedicals, Heidelberg, Germany), Mg^{2+} and Ca^{2+} free phosphate buffered saline (PBS) (Biochrome, Berlin Germany), N-(3-triethylammoniumpropyl) -4-(4-(dibutylamino)styryl) pyridinium dibromide (FM1-43), Lysotracker red (LTR), Fura-2-AM ester (Fura-2) and Fluo-4-AM ester (Fluo-4) were from Invitrogen Molecular Probes (Karlsruhe, Germany). Other chemicals were purchased from Sigma Aldrich (Munich, Germany).

Solutions and reagents

Bath solution (BS) contained, in mM, 140 NaCl, 5 KCl, 1 $MgCl_2$, 2 $CaCl_2$, 5 glucose, and 10 HEPES (pH 7.4 at 25°C). Calcium free BS was prepared by omitting the calcium and adding 10 mM EGTA. Brilliant Black was added to Bath solution at a concentration of 2 mg/ml to block background fluorescence [19]. Unless otherwise mentioned all the blockers were incubated for 20 to 30 min at 37°C and remained in the solution during the whole duration of experiment.

Cell culture of NCI-H441 cells

H441 cells were obtained from American Type Culture Collection, (Manassas, VA) and grown in RPMI 1640 medium supplemented with 10% fetal bovine serum, sodium pyruvate, penicillin (100 units/ml) and streptomycin (100 µg/ml). Cells were seeded in 25-cm^2 flasks and incubated in a humidified atmosphere of 5% CO_2 at 37°C until they reached 90% confluence and cells were passaged every week. Cells were trypsinized and seeded at a density of 10^4 cells/well on 96-well tissue culture plates and grown for 2-3 days before using them for experiments. The medium was changed every other day.

Isolation and cultivation of ATII cells

Alveolar type II (ATII) cells were isolated from male sprague dawley rats as described [20]. Briefly, rats of 180 to 200 g weight were anesthetized, anticoagulised and lungs were cleared by perfusion. After lavage, lungs were instilled twice with wash solution containing elastase (30 U/ml) and trypsin (2 mg/ml) at 37°C. Lungs were minced in the presence of DNase and fetal calf serum (FCS) and cell suspension was sequentially filtered through cotton gauze and nylon meshes. Cells were centrifuged and resuspended in DMEM. Macrophages were removed by panning cell suspension to IgG coated Petri dishes at 37°C. The unattached cells were removed, pelletized by centrifugation and resuspended in DMEM with 10% FCS, 100 units/ml penicillin, 100 µg/ml streptomycin, and 24 mM $NaHCO_3$ (growth medium). Cells were used after 2 days in culture.

Fluo-4 measurement in H441 cells

H441 cells were incubated with 3 µM Fluo-4 for 30 min at 37°C in a humidified atmosphere of 5% CO_2. After replacing the medium with brilliant black containing bath solution, cells were placed into a Tecan Infinite 200 microplate reader (Tecan AG, Switzerland) and kinetic cycle was started with excitation and emission at 490 nm and 525 nm respectively. Cells were stimulated after fluorescence reached a steady state. Compounds were added as 2 fold concentrated solutions in bath solution with brilliant black directly onto the cells and kinetic cycle was continued for another 20 minutes. Data acquisition was done with Tecan i-control software version 1.1.9.0 and analyzed using Microsoft Excel. Relative fluorescence units (RFU) were

calculated as fluorescence intensities normalized to fluorescence intensity measured at the last time point before compound application. Peak RFU implies to the maximal measured RFU after compound application. Steady state RFU was calculated as mean RFU over the last five time points after compound application, when fluorescence intensities reached steady state. All the measurements were performed in triplicates.

Fura-2 measurements in ATII cells

ATII cells cultured on ibidi µ-Dishes (35 mm, low) for 2 days were loaded with 3 µM Fura-2-AM ester for 15- 20 min at 37°C for intracellular Ca^{2+} measurements on a Zeiss Cell observer equipped with a cool snap EZ CCD camera. Images were acquired with Fluar 40x/1.3 oil objective (Zeiss, Göttingen Germany), using Metamorph image acquisition software package version 7.5.5.0 (Visitron Systems GmbH, Pucheim Germany). Cells were excited at 340 and 380 nm using a monocromator (Visitron Systems GmbH) and images were acquired every 2 seconds for a total duration of 10 minutes. Ratiometric analysis was performed using newest version of ImageJ software (version 1.42l, National Institute of Health, USA, http://rsb.info.nih.gov/ij).

FM1-43 uptake by H441 cells

Semi-confluent H441 cells cultured on ibidi µ-Dishes (35 mm, low) were imaged for 3 µM FM1-43 uptake on a Zeiss Cell observer equipped with a cool snap EZ CCD camera. Images were acquired using LD Plan-NEOFLUAR 40x/0.6 Ph2 Korr objective, FM1-43 filter and Metamorph software. Cells were incubated with FM1-43 and 2-APB & CPZ containing bath solution using an in-house built perfusion chamber for 30 min and images were acquired every 20 s before and after washout of FM1-43. Images were analysed offline using newest version of ImageJ software.

In addition to microscopical investigation, FM1-43 uptake was quantified using Tecan Infinite 200 microplate reader. H441 cells were incubated with the FM1-43 in the presence or absence of compounds for 25-30 min at 37°C. After replacing the medium with brilliant black containing bath solution, the cells were placed into Tecan Infinite 200 microplate reader. FM1-43 internalised by the cells, was fluorometrically quantified by exciting the cells at 480 nm and collecting fluorescence at 590 nm.

FM1-43 uptake by ATII cells

ATII cells cultivated in 8 well µ-slides were washed with BS and were pre-incubated prior to the experiments in BS at room temperature (21°C to 23°C, RT) with FM1-43 and mounted afterwards on the microscope. Representative groups of cells were selected and imaging was carried out on a Zeiss Cell observer equipped with a LD Plan-NEOFLUAR 40x/0.6 Ph2 Korr objective and an EZ CCD-camera (Excitation 450 - 490 nm, dichroic filter 495 nm and emission 500 - 550 nm). Metamorph software package version 7.5.5.0 (Visitron Systems GmbH) was used for x/y/z-positioning and data acquisition. For cell stimulation 2-APB, CPZ or 2-APB/CPZ were added directly to the cells. Perinuclear fluorescence intensities were measured after background subtraction using ImagJ software and were normalised to the intensity measured at the first time point after compound application in order to calculate relative fluorescence intensities (RFU).

Semi-thin slices of ATII cells

ATII cells were cultivated for 2 days on glass cover slips and were washed twice with BS. Cells were incubated with or without 2-APB/CPZ for 20 min at RT in BS. Afterwards, cells were fixated using PBS containing 2.5% glutaraldehyde and 1% sucrose followed by 1 hour incubation in PBS containing 2% OsO_4 followed by dehydration of cells by bathing in a stepwise increased alcohol concentration and Epon embedding of cells. Semi-thin sections of 500 nm thickness were obtained using an ultramicrotome (Leica, Bensheim Germany). Sections were mounted on glass slides and microscopically investigated.

Statistic analysis

Data are presented as Mean ± SEM. Statistical significance was determined with unpaired two tailed students t-test and statistical significance was assigned when $P \leq 0.05$ and indicated with $^{**}P \leq 0.05$.

Results

2-APB and CPZ induced Ca^{2+} entry

We tested initially the effect of TRP and SOC channel inhibitors (Fig. 1 A, B) and activators (Fig. 1 C, D) on cytoplasmic Ca^{2+} concentration ($[Ca^{2+}]_c$). Although CPZ is commonly considered as a TRPV1 channel blocker [21] it elevated $[Ca^{2+}]_c$. A similar effect was observed for 2-aminoethoxy-di-phenyl-borinate (2-APB). For both compounds the $[Ca^{2+}]_c$ increasing effect was concentration dependent (Fig. 2). A decrease in $[Ca^{2+}]_c$ was observed after application of capsaicin, an activator of TRPV1 channels and 4αPDD, an activator of TRPV4 channels (Fig. 1). This observation can not be explained by a direct interaction of these compounds with their target channel but might reflect unspecific side effects in these cells. 2-APB induced a biphasic response with similar threshold concentrations for both phases (Fig. 2 A, B). Contrary to 2-APB, CPZ induced a delayed and monophasic $[Ca^{2+}]_c$ increase (Fig. 2 C, D).

When 2-APB and CPZ were applied simultaneously to the bath solution a biphasic $[Ca^{2+}]_c$ elevation was observed (Fig. 3A). The $[Ca^{2+}]_c$ increase was completely abolished, when cells were preloaded with the Ca^{2+} chelator BAPTA-AM, but also when extra-cellular Ca^{2+} was depleted or when SKF96365 was present in the bath solution (Fig. 3 A, B). The fact that $[Ca^{2+}]_c$ elevation was completely abolished by extra-cellular Ca^{2+} depletion indicates that 2-APB/CPZ activated a Ca^{2+} entry path-

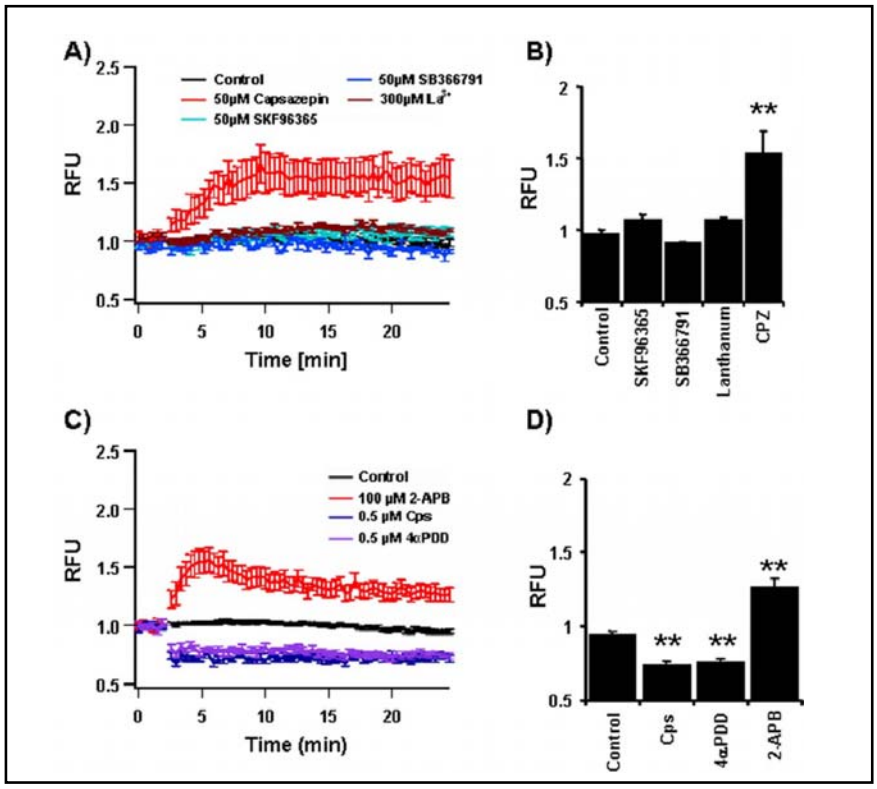

Fig. 1. Effect of known modulators of Ca^{2+} entry pathways in H441 cells. Changes in $[Ca^{2+}]_c$ were measured using Fluo-4 in a plate reader assay. Fluorescence intensities were given as relative fluorescence units (RFU). A) Time course of $[Ca^{2+}]_c$ changes induced by 50 µM SKF96365, 50 µM SB366791, 50 µM Capsazepine (CPZ) and 300 µM La^{3+}. B) Bar diagram represents steady state RFU observed after application of compounds shown in A. (all values given as mean ± SEM, N = 12) C) Time course of $[Ca^{2+}]_c$ changes induced by 100 µM 2-aminoethoxydiphenylborinate (2-APB), 0.5 µM Capsaicin (Cps) and 0.5 µM 4-phorbol 12,13-didecanoate (4αPDD). D) Bar diagram represents steady state RFU observed after application of compounds given in C (all values given as mean ± SEM , N = 9). Asterisk denotes statistical significance vs control.

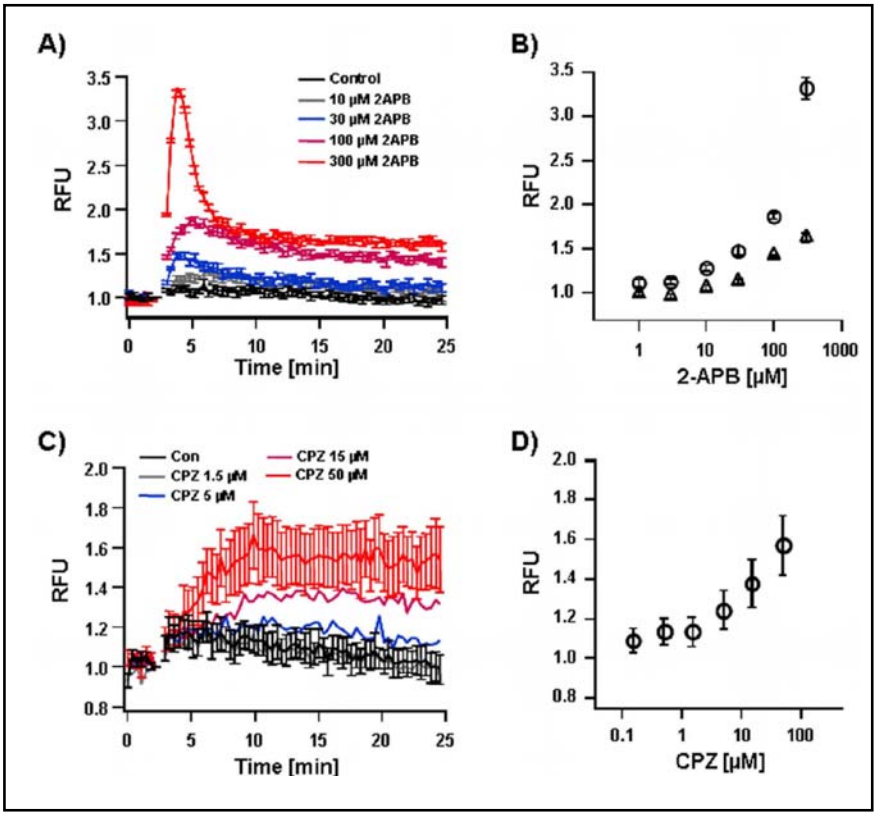

Fig. 2. 2-APB and CPZ increase $[Ca^{2+}]_c$ in a concentration dependent manner in H441 cells. $[Ca^{2+}]_c$ was measured using Fluo-4 in a plate reader assay. Fluorescence values are given as relative fluorescence units (RFU). A) Time course of $[Ca^{2+}]_c$ after application of 2-APB at given concentrations. For clarity 1 µM and 3 µM 2-APB are omitted as they do not show any effects. B) RFU is plotted against 2-APB concentrations. Open circles = maximum RFU measured as highest RFU, open triangles = steady state RFU measured as mean RFU over the last five time points of each experiment. Both steady state and peak RFU increase at concentrations above 3 µM. C) Time course of $[Ca^{2+}]_c$ after application of CPZ at given concentrations. For better clarity, error bars are given only for control cells and cells stimulated at the highest tested CPZ concentration also 0.15 and 0.5 µM are omitted since CPZ did not show any effect at these concentrations. D) RFU is plotted against the CPZ concentration. (For all experiments values are given as mean ± SEM, N = 6)

way. Consistent with the lack of L-type Ca^{2+} channels [22], nifedipine and verapmil had no effect on the induced $[Ca^{2+}]_c$ increase (data not shown).

The Ca^{2+} influx induced by 2-APB does not differ in its pharmacological properties from the influx induced by CPZ (Fig. 4). Both influx pathways remained unaffected by La^{3+} and SB366791 but were completely abolished by SKF96365.

For cells stimulated with 2-APB/CPZ, SKF96365 affected both phases of Ca^{2+} influx (Fig. 5). The

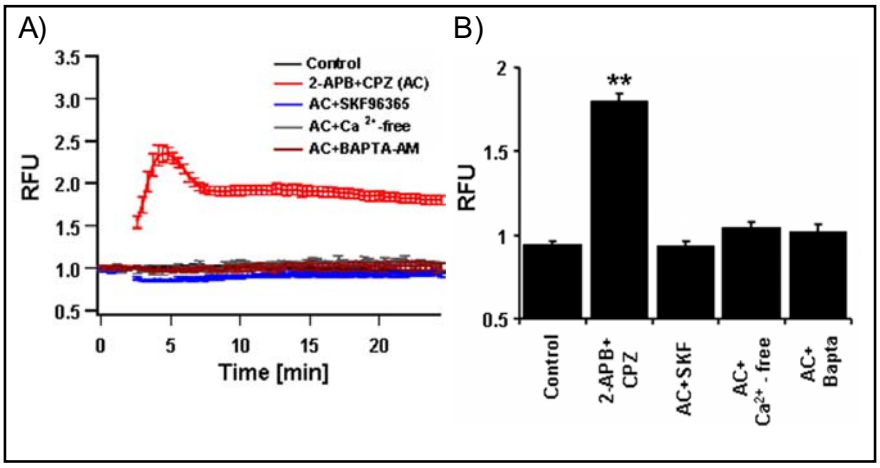

Fig. 3. 2-APB/CPZ induced $[Ca^{2+}]_c$ increase depends on Ca^{2+} influx in H441 cells. $[Ca^{2+}]_c$ was quantified using Fluo-4. Fluorescence intensities are given as relative fluorescence units (RFU) A) Time course of $[Ca^{2+}]_c$. Control = untreated control cells, 2-APB/CPZ = cells stimulated by 100 µM 2-APB and 50 µM CPZ, AC + compound/treatment = 2-APB/CPZ treated cells in the presence of 100 µM SKF96365, in the absence of Ca^{2+} or after preloading using the Ca^{2+} chelator BAPTA-AM. B) Steady state RFU after cell stimulation from experiments summarised in A. Asterisks denote statistical significance versus control.

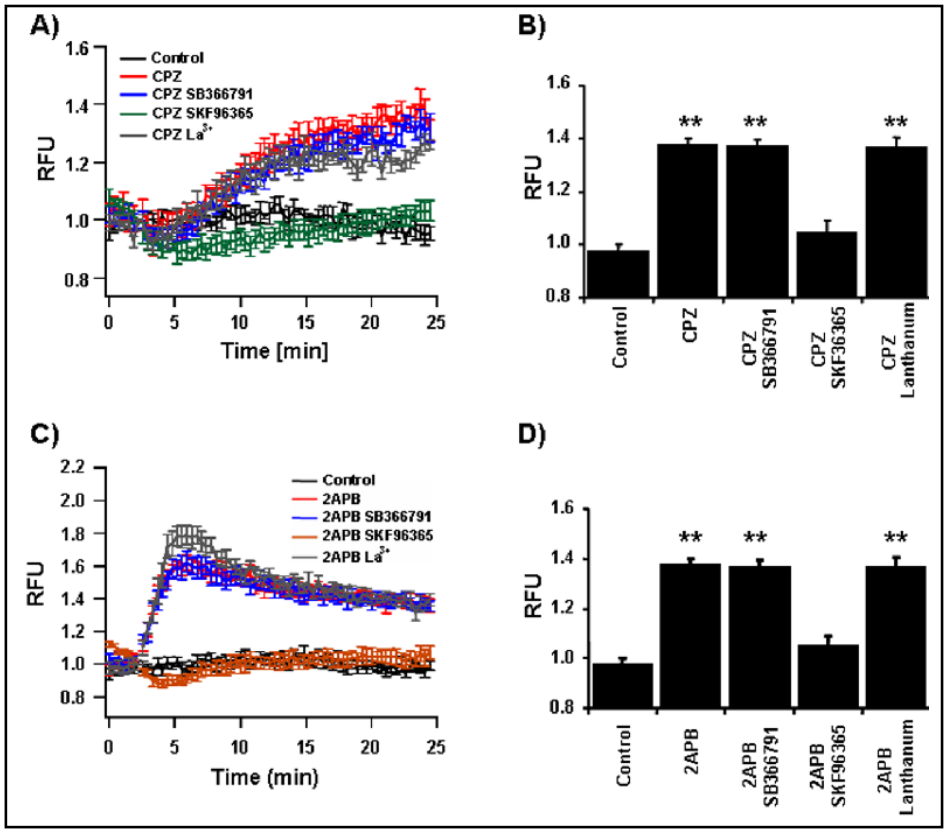

Fig. 4. Pharmacological properties of Ca^{2+} influx induced by CPZ and 2-APB in H441 cells. $[Ca^{2+}]_c$ were measured using Fluo-4. Fluorescence intensities are given as relative fluorescence units (RFU). Time course of $[Ca^{2+}]_c$. A) Capsazepine stimulation (control = control cells, CPZ = cells stimulated by 50 µM CPZ, CPZ+compound name = cells stimulated by CPZ in the presence of 5 µM SB366791, 100 µM SKF96365 or 300 µM La^{3+}) C) 2-APB stimulation (control = control cells, 2-APB = cells stimulated by 50 µM 2-APB, 2-APB+compound name = cells stimulated by 2-APB in the presence of 5 µM SB366791, 100 µM SKF96365, 300 µM La^{3+}). B and D) Bar charts represent steady state RFU for experiments summarised in A and C respectively. Asterisks denote statistical significance versus control.

transient phase was blocked in a concentration dependent manner (Fig. 5B), whereas the sustained component was potentiated at concentrations below 10 µM and blocked at concentrations of 10 µM and above (Fig. 5C). Contrary to SKF96365, La^{3+} (Fig. 5 D, E) and SB366791 (Fig. 5 F, G) affected the transient component only. La^{3+} blocked the transient phase in a concentration dependent manner, whereas SB366791 potentiated the transient Ca^{2+} influx pathway at concentrations below 0.3 µM and blocked it at concentrations of 0.3 µM and above.

The effect of 2-APB/CPZ stimulation was also tested on primary cultivated ATII cells (Fig. 6). Although these cells lacked a clear biphasic Ca^{2+} response upon stimulation, the pharmacological profile of inhibition of Ca^{2+} entry was similar to that observed in H441 cells (Fig. 5).

2-APB/CPZ induced clathrin dependent endocytosis

Since Ca^{2+} signaling in epitheloid cells was recently associated with the internalization of aquaporins [5, 23-25], we tested the effect of 2-APB/CPZ on a possible internalization of plasma membrane components. Therefore, we investigated the uptake of FM1-43 from the extra-cellular space, a well established method to study

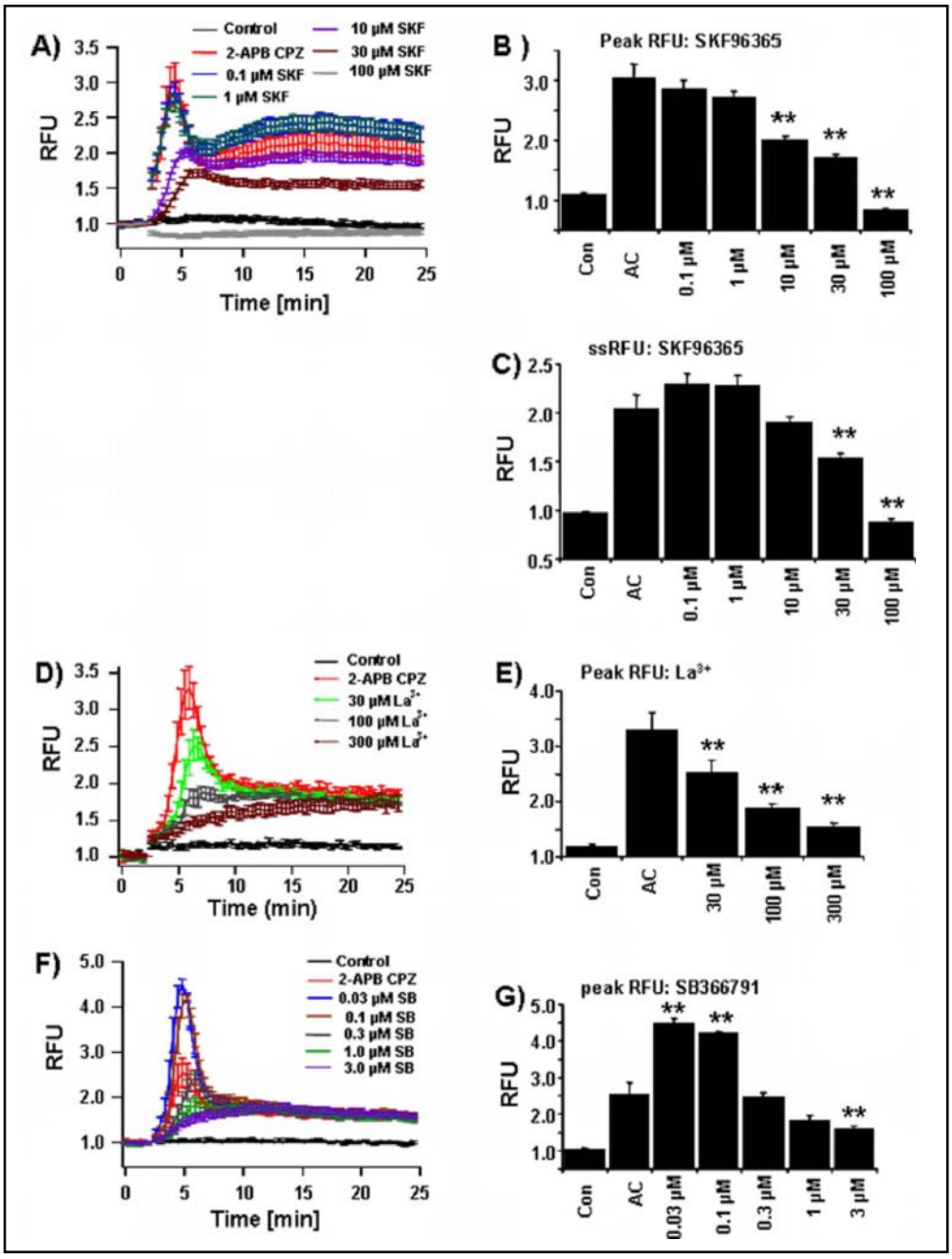

Fig. 5. Pharmacological properties of 2-APB/CPZ induced Ca^{2+} influx. A) Time course of $[Ca^{2+}]_c$ in 2-APB/CPZ stimulated cells in the presence of SKF96365 at assigned concentrations. B) Peak RFU measured as maximum RFU and C) steady state RFU from experiments summarised in A. D) Time course of $[Ca^{2+}]_c$ in 2-APB/CPZ stimulated cells in the presence of La^{3+} at given concentrations. E) Peak RFU measured as maximum RFU summarised in D. F) Time course of $[Ca^{2+}]_c$ in 2-APB/CPZ stimulated cells in the presence of SB366791 at given concentrations G) Peak RFU measured as maximum RFU from experiments summarised in F. Steady state RFU were not affected by La^{3+} and SB366791 and therefore not shown in bar diagrams. Asterisks denote statistical significance versus 2-APB/CPZ stimulated cells. (Con = untreated control cells, 2-APB/CPZ = cells stimulated by 100 µM 2-APB and 50 µM CPZ.)

endocytosis [26]. At the beginning of each experiment, FM1-43 labeled the plasma membrane of H441 cells under control conditions (Fig. 7 A, B). This signal was reversible upon removal of FM1-43 from the extra-cellular solution (Fig. 7B), consistent with its reversible incorporation into the plasma membrane outer leaflet [26]. When cells were stimulated by 2-APB/CPZ, the FM1-43 fluorescence was observed peri-nuclearly and remained there even after FM1-43 removal from the bath solution (Fig. 7D).

In order to investigate FM1-43 uptake mechanisms in 2-APB/CPZ stimulated H441 cells, we quantified FM1-43 uptake using a plate reader assay. The results are summarized in Fig. 7 E and show that the pharmacological profile of FM1-43 uptake strongly correlates to the changes in $[Ca^{2+}]_c$ described above. This together with the observation that Ca^{2+} depletion from the bath solution as well as preloading of cells with the Ca^{2+} chelator BAPTA-AM inhibited FM1-43 uptake indicates that the this uptake of FM1-43 is mediated via 2-APB/CPZ induced $[Ca^{2+}]_c$ elevation. In order to test for uptake mechanism, H441 cells were incubated with several blockers of endocytosis prior to 2-APB/CPZ stimulation. Exposure of cells to 4°C and treatment by phenylarsine oxide (PAO), a blocker of clathrin-dependent endocytosis [27-29] abolished FM1-43 uptake. In contrast, blockers of

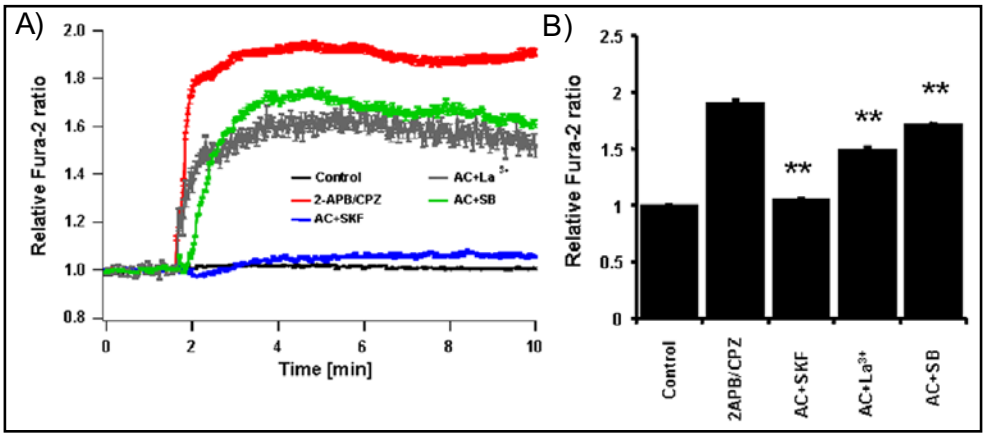

Fig. 6. Fura-2 measurements in ATII cells. ATII cells were loaded with Fura-2-AM as a Ca^{2+} sensing dye. Fluorescence intensity was measured at excitation wave length 340 nm and 380 nm. After calculating Fura-2 ratio, values were normalised to base line value measured before stimulation of cells by 2-APB/CPZ (relative Fura-2 ratio). A) Values shown in the diagram represents mean relative Fura-2 ratios ± SEM. Control = non-stimulated control cells, 2- APB/CPZ = cells stimulated by 2-APB/CPZ, AC+SKF = cells stimulated by 2-APB/CPZ in the presence of 100 µM SKF96365, AC+La^{3+} = cells stimulated by 2-APB/CPZ in the presence of 300 µM La^{3+} and AC+SB = cells stimulated by 2-APB/CPZ in the presence of 5 µM SB366791. B) Bar diagram represents steady state Fura-2 ratios normalised to baseline. Abbreviations as in A. Asterisk denotes statistical significance vs 2-APB/CPZ.

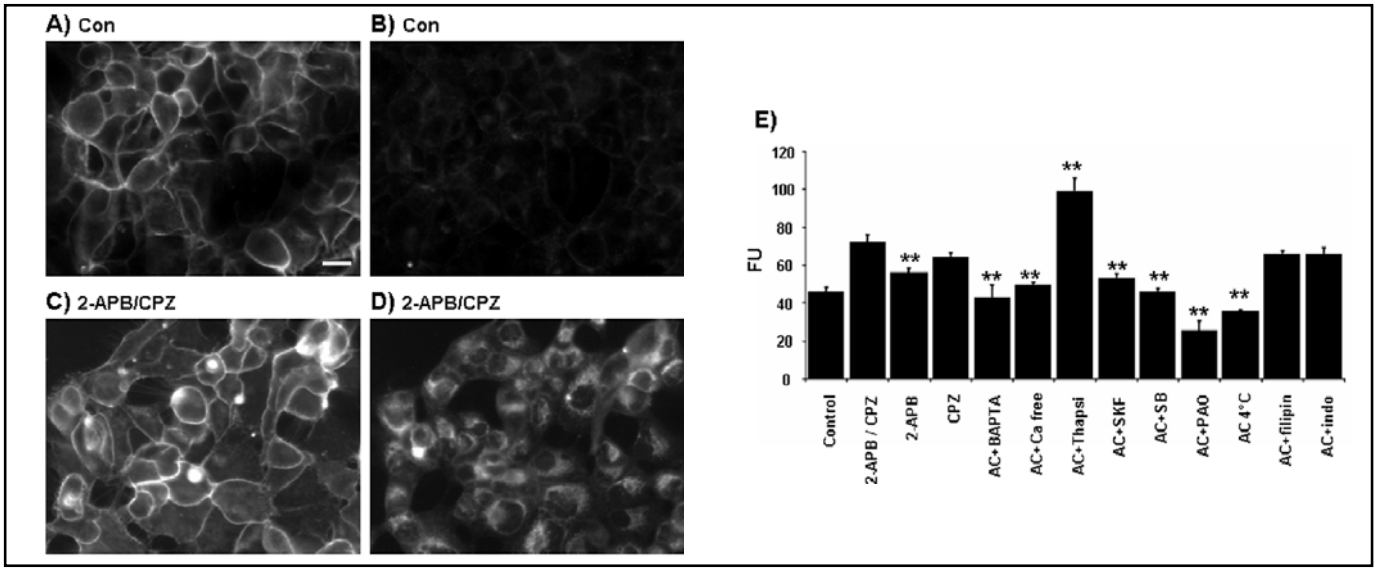

Fig. 7. FM1-43 uptake in H441 cells induced by 2-APB/CPZ. Cells were incubated with the ambiphilic membrane dye FM1-43 and stimulated afterwards for 25 min by 2-APB/CPZ. FM1-43 internalised by cells upon 2-APB/CPZ stimulation remained fluorescent inside the cells, whereas non internalised FM1-43 dye remained in the plasma membrane was removed from cells after wash out (Scale bar 20 µm). A and B) Un-stimulated control cells after FM1-43 loading and after washout respectively. C and D) 2-APB/CPZ stimulated cells after FM1-43 loading and after wash out respectively. E) FM1-43 uptake was quantified by plate reader assay. H441 cells were cultivated in 96 well plates. Internalised FM1-43 was quantified as arbitrary fluorescence units (FU) and values are represented in the bar diagram as mean FU ± SEM (Control = non-stimulated control cells, 2-APB/CPZ = cells stimulated by 2-APB/CPZ (100 µM/50 µM respectively), 2-APB = cells stimulated by 100 µM 2-APB, CPZ = cells stimulated by 50 µM CPZ, AC+BAPTA = cells stimulated by 2-APB/CPZ after preloading with the Ca^{2+} chelator BAPTA-AM, AC+Ca^{2+} free = cells stimulated by 2-APB/CPZ in the absence of extra-cellular Ca^{2+}, AC+Thapsi = cells stimulated by 2-APB/CPZ in the presence of Thapisgargin, AC+SKF = cells stimulated by 2-APB/CPZ in the presence of 100 µM SKF96365, AC+SB = cells stimulated by 2-APB/CPZ in the presence of 50 µM SB366791, AC+PAO = cells stimulated by 2-APB/CPZ in the presence of 10 µM PAO, AC 4°C = cells stimulated by 2-APB/CPZ at 4°C, AC+filipin = cells stimulated by 2-APB/CPZ in the presence of 5 µM filipin, AC+indomethacin = cells stimulated by 2-APB/CPZ in the presence of 150 µM indomethacin). Asterisk denotes statistical significance vs 2-APB/CPZ.

clathrin-independent endocytosis, such as indomethacine and filipin [30-32] had no effect on 2-APB/CPZ induced FM1-43 uptake.

Similar phenomenon was also observed for ATII cells upon stimulation with 2-APB/CPZ (Fig. 8). To investigate the intracellular distribution of FM1-43, ATII

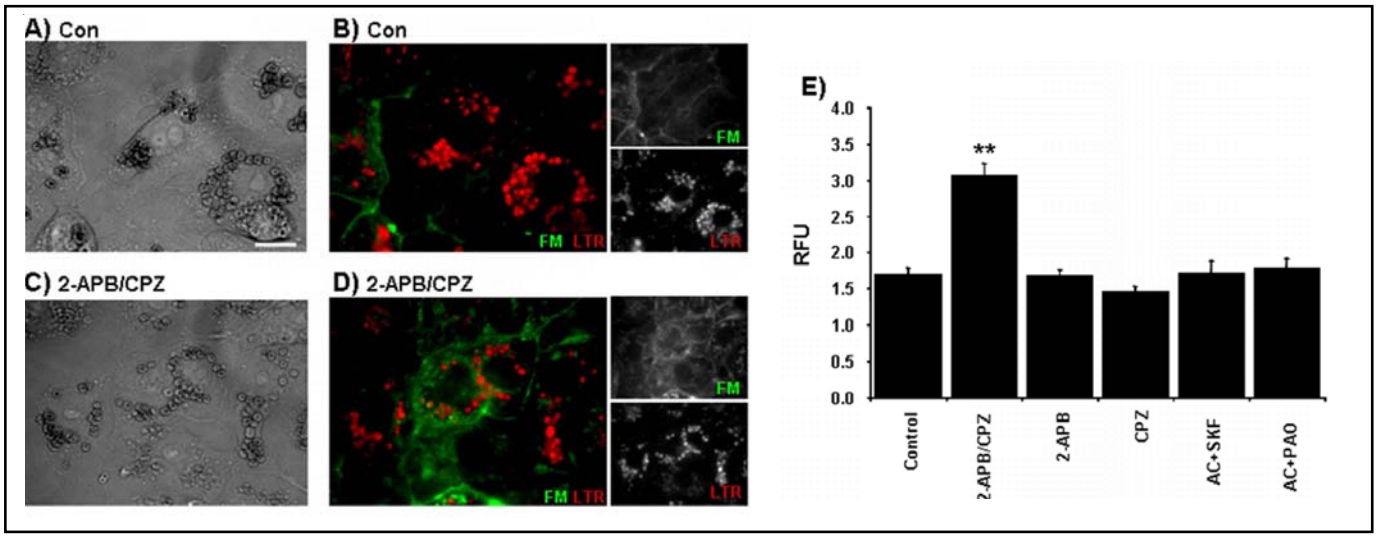

Fig. 8. FM1-43 uptake in ATII cells induced by 2-APB/CPZ. ATII cells were incubated in bath solution containing FM1-43 for 25 min. A, B) Control cells remained untreated (Scale bar 20 µM). C, D) Cells were stimulated by application of 100 µM 2-APB+50 µM CPZ (2-APB/CPZ). Phase contrast images (A, C) and epifluorescence images (B, D) of living cells were taken after FM1-43 (FM, green fluorescence channel) washout and LB labelling by lysotracker red (LTR, red fluorescence channel). Small insets at the right represents grey scale images for both fluorescence channels. E) Quantification of FM1-43 uptake. ATII cells were cultivated on an 8-well µ-Slide, incubated in bath solution containing FM1-43 and mounted on a microscope. Representative groups of cells were selected and imaged. Perinuclear fluorescence intensities were measured from grey scale images. Relative fluorescence units (RFU) were calculated as values normalised to the first value directly after compound application. Bar diagram represents mean RFU±SEM after 25 min incubation. Control = control cells, 2-APB/CPZ = cells stimulated by 100 µM 2-APB/50 µM CPZ, 2-APB = cells in the presence of 100 µM 2-APB, CPZ = cells in the presence of 50 µM CPZ, AC+SKF = cells stimulated by 2-APB/CPZ in the presence of 100 µM SKF96365, AC+PAO = cells stimulated by 2-APB/CPZ in the presence of 10 µM PAO. Asterisks denote statistical significance versus 2-APB/CPZ stimulated cells.

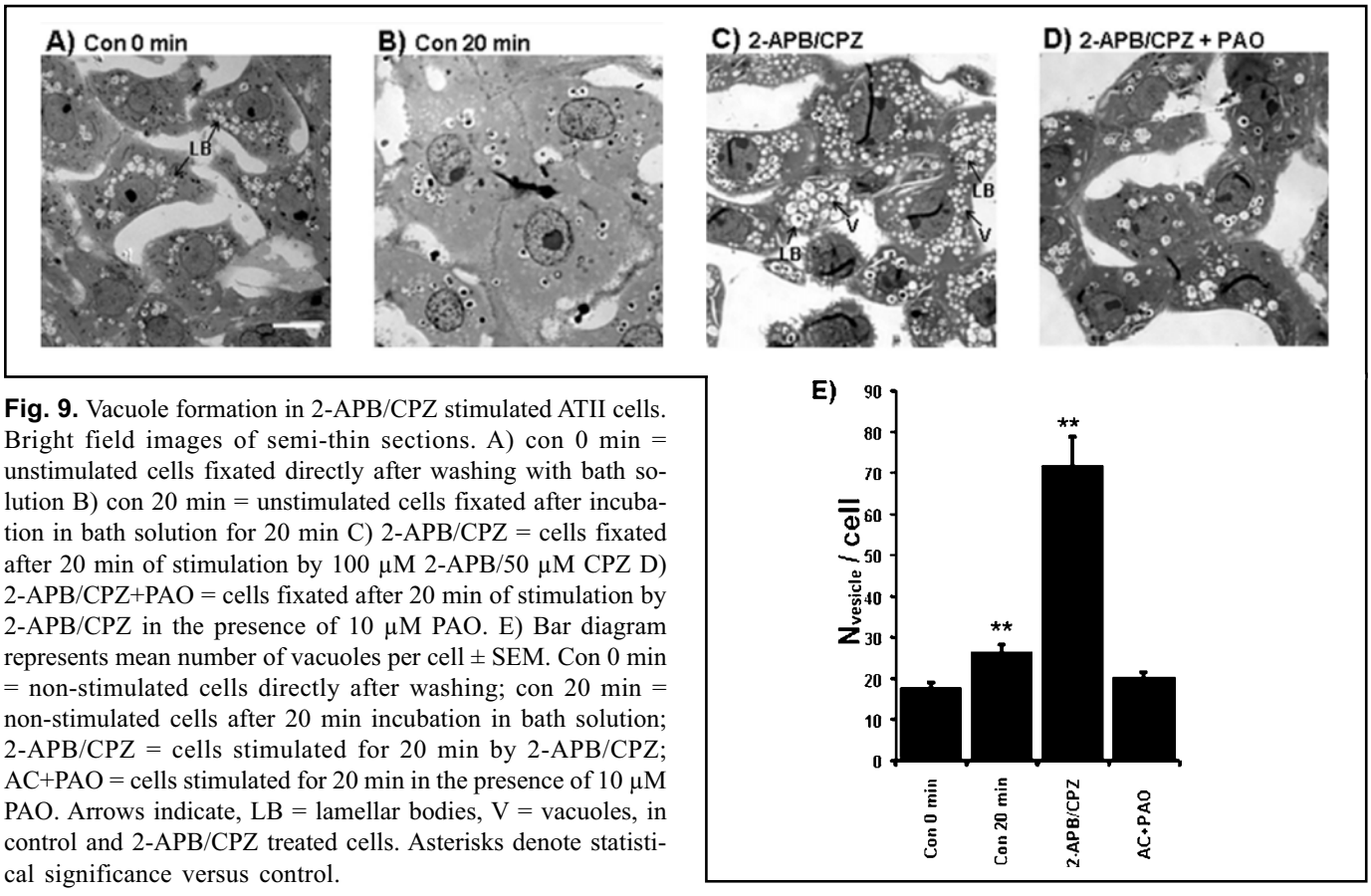

Fig. 9. Vacuole formation in 2-APB/CPZ stimulated ATII cells. Bright field images of semi-thin sections. A) con 0 min = unstimulated cells fixated directly after washing with bath solution B) con 20 min = unstimulated cells fixated after incubation in bath solution for 20 min C) 2-APB/CPZ = cells fixated after 20 min of stimulation by 100 µM 2-APB/50 µM CPZ D) 2-APB/CPZ+PAO = cells fixated after 20 min of stimulation by 2-APB/CPZ in the presence of 10 µM PAO. E) Bar diagram represents mean number of vacuoles per cell ± SEM. Con 0 min = non-stimulated cells directly after washing; con 20 min = non-stimulated cells after 20 min incubation in bath solution; 2-APB/CPZ = cells stimulated for 20 min by 2-APB/CPZ; AC+PAO = cells stimulated for 20 min in the presence of 10 µM PAO. Arrows indicate, LB = lamellar bodies, V = vacuoles, in control and 2-APB/CPZ treated cells. Asterisks denote statistical significance versus control.

cell were stimulated in presence of FM1-43, followed by FM1-43 washout and labelling of LB by acidotrophic dye lysotracker red (LTR). In these experiments (Fig. 8A-D) internalized FM1-43 accumulated juxtanuclearly to granules distinct from LBs.

When LBs fuse with the plasma membrane, FM1-43 entry into the LB lumen via the exocytotic fusion pore causes a bright localized LB staining, according to the lipid-induced quantum yield of FM1-43 [33]. We used this approach to quantify FM1-43 uptake in ATII cells without depleting FM1-43 from the bath solution under microscopic observation, since this allowed us to identify LB fusion and to quantify FM1-43 uptake via endocytosis at the same time. The stimulation of ATII cells by 2-APB/CPZ did not induce surfactant exocytosis, since surfactant exocytosis was observed in 4.4 % of control cells (N = 182) and in 4.1% of 2-APB/CPZ stimulated cells (N = 49). The pharmacological properties of FM1-43 uptake in ATII cells resemble the properties of the 2-APB/CPZ induced Ca^{2+} entry (Fig. 8 E) as it was observed for H441 cells. FM1-43 uptake in ATII cells was also blocked completely by PAO. Thus we show that 2-APB/CPZ stimulation induces clathrin dependent endocytosis in both cell types via $[Ca^{2+}]_c$ elevation.

2-APB/CPZ induced vacuole formation in ATII cells

Since internalized FM1-43 appeared to be localized at granular structures in ATII cells (Fig. 8 D), we investigated if 2-APB/CPZ stimulation induces also changes in intracellular compartments (Fig. 9). In semi-thin slices of fixated control cells, ATII cells typically exhibit vacuoles which are organized concentrically around the nucleus and which contain some dense material. These vacuoles correspond to lamellar bodies, which are the typical surfactant storing vesicles in ATII cells (Fig. 9 A, B). ATII cells stimulated by 2-APB/CPZ for 20 min exhibited a dramatically increased number of vacuoles (Fig. 9C), which was not observed in PAO treated cells (Fig. 9D) giving evidence that the vacuole formation is associated with clathrin mediated endocytosis. In contrast to control cells, 2-APB/CPZ treated ATII cells exhibit two different types of vacuoles. One type of vacuoles, which is similar to control cells, and contains an optical dense material inside their lumen and a second type, which is lacking such material and can be assumed as formed upon 2-APB/CPZ stimulation. The pattern of vacuoles in stimulated ATII cells resembles the fluorescence pattern of FM1-43, taken up upon 2-APB/CPZ treatment. However, a slight but statistically significant increased number of vacuoles was observed in ATII cells kept under control conditions for 20 min (Fig. 9B). This observation could be easily explained by basal endocytosis in these cells. This increase in number of vacuoles can effectively be blocked by PAO treatment, which again suggests that even the basal endocytosis is dependent on clathrin.

Discussion

Calcium entry in ATII cells is an essential component of both agonist [3] and strain induced [2] surfactant exocytosis. Even though the importance of Ca^{2+} signaling in ATII cells for surfactant exocytosis and respiratory function is widely accepted, Ca^{2+} signaling pathways are still poorly understood in these cells.

While aiming to elucidate Ca^{2+} entry pathways in distal airway epithelial cells we made the surprising finding that the two investigated $[Ca^{2+}]_c$ modulators 2-APB and CPZ not only stimulate Ca^{2+} entry in ATII and NCI-H441 cells but also induce substantial clathrin dependent endocytosis. So far, $[Ca^{2+}]_c$ elevation in ATII cells was predominantly discussed as a modulator for surfactant exocytosis [2, 3]. Herein we demonstrate that the 2-APB/CPZ activated increase in $[Ca^{2+}]_c$ causes clathrin dependent endocytosis instead of LB exocytosis.

2-APB is a commonly used compound for investigating Ca^{2+} signaling pathways in different cell types. It was recently described as a membrane permeable compound, which inhibits Ca^{2+} release from intra-cellular stores via inhibition of Ins(1,4,5)P3 receptors [34]. In a later study it became evident, that 2-APB blocks Ca^{2+} entry via a direct interaction with store operated Ca^{2+} (SOC) channels [35, 36]. On the other hand, 2-APB was shown to act as a partial activator on store operated Ca^{2+} entry [36, 37]. This heterogeneity in mode of action for 2-APB on SOC mediated Ca^{2+} influx pathways has been shown to depend on the molecular diversity of SOC channels. These channels consist of the regulatory subunits STIM1 and STIM2 [6] and their interacting pore forming protein partners Orai1, -2 and -3 [6-9, 38]. They form either homomeric or heteromeric protein complexes with distinct biophysical and pharmacological properties [10]. STIM1/Orai1 and STIM1/Orai2 mediated currents are potentiated by 2-APB at concentrations below 20 μM but are completely blocked by 50 μM 2-APB. STIM1/Orai3 currents are in turn activated even at 2-APB concentrations above 50 μM [39]. Beside an activator of SOC channels 2-APB is also reported to activate TRPV1, -V2 and -V3 channels [40]. We also demonstrated that

capsazepine (CPZ), a synthetic TRPV1 inhibitor [21], also elevated $[Ca^{2+}]_c$ via Ca^{2+} entry. Taking into account, that the interaction of TRP channel and Orai/STIM subunits could also be involved in SOC channels formation [15], someone would expect a diverse family of possibly 2-APB and maybe also CPZ modulated Ca^{2+} entry pathways. Those possibilities could explain the observed elevation in $[Ca^{2+}]_c$ demonstrated in our study. However, SOC [41, 42] as well as TRP [43] channels are sensitive to La^{3+} and SKF96365. Our observation that SKF96365 but not La^{3+} blocked both 2-APB/CPZ activated Ca^{2+} influx pathways makes it unlikely that a single classical SOC or TRP channel would be involved in this process. Furthermore, we also found that 2-APB alone and 2-APB/CPZ blocked thapsigargin induced Ca^{2+} entry (data not shown). This indicates that 2-APB/CPZ blocks SOC rather than activating it.

When 2-APB and CPZ were applied together to H441 cells, a biphasic $[Ca^{2+}]_c$ increase was observed. The two different phases can be subdivided into a transient and a sustained component. Both components have different pharmacological properties. SB366791 is reported as a highly selective and potent inhibitor of TRPV1 channels [44]. Therefore our observation that the transient Ca^{2+} influx pathway is sensitive to SB366791 could suggest that it might be mediated via TRPV1 channels. However, the transient Ca^{2+} signal was activated in the presence of 50 μM CPZ, a concentration approximately 100 fold higher than the IC_{50} value reported for the CPZ blockage of human TRPV1 channels [45]. Thus, a contribution of TRPV1 channels in mediating the transient $[Ca^{2+}]_c$ elevation is very unlikely.

The pharmacological properties of the transient phase of Ca^{2+} influx resemble those properties already described for several SOC channels [41]. Experiments in which the extra-cellular Ca^{2+} was depleted 2-APB/CPZ did not activate any Ca^{2+} release from intra-cellular stores. Also the fact that 2-APB/CPZ blocked thapsigargin induced SOC entry clearly contradicts the possibility that the sustained component of $[Ca^{2+}]_c$ increase could be mediated via SOC channels.

In ATII cells 2-APB/CPZ stimulated a $[Ca^{2+}]_c$ increase, which differed at least in its time course from the $[Ca^{2+}]_c$ elevation in H441 cells. However, the observation that SB366791 and La^{3+} abolished $[Ca^{2+}]_c$ increase only partially, whereas it was completely blocked by SKF96365 is common for both cell types and gives evidence for two different mechanisms for $[Ca^{2+}]_c$ also in ATII cells.

The incubation of ATII and H441 cells with 2-APB/CPZ facilitated clathrin dependent endocytosis of FM1-43 via $[Ca^{2+}]_c$ elevation. Even if ATII cells differ in their Ca^{2+} response to 2-APB/CPZ treatment from H441 cells, the Ca^{2+} mediated endocytosis is a common mechanism observed for both cell types. However, the fluorescence pattern of internalized FM1-43 appears more granulated in ATII cells than it was observed in H441 cells. Furthermore, in ATII cells internalized FM1-43 localized to non acidic organelles. Organelle acidification is an essential step for an appropriate sorting and trafficking of internalized material and occurs even at the stage of the early endosome [46]. Therefore, the observed accumulation of FM1-43 in non-acidic organelles might be explained by an insufficient processing of internalized material at a stage preceding entry into late endosome. This would also explain the observed vacuole formation, since an extraordinarily increased accumulation of material inside an organelle would also result in an increased organelle size.

Endocytosis in ATII cells was shown to be involved in recycling of lamellar body associated proteins but also in surfactant uptake from extra-cellular space [47, 48]. Especially, the surfactant uptake is predominantly dependent on clathrin mediated endocytosis in ATII cells. However, Ca^{2+} signaling in ATII cells was until now implicated in regulation of LB fusion and exocytosis of surfactant [3] but not endocytosis in ATII cells. Nevertheless, there are several lines of evidence that Ca^{2+} could modulate endocytosis in epithelial cell types. Ca^{2+} has been shown to mediate the formation of protein complexes, which initiates clathrin accumulation at the side of internalization in different cell types [49, 50]. Furthermore, changes in $[Ca^{2+}]_c$ in epitheloid cells were recently demonstrated to modulate the protein composition of plasma membrane via regulated endocytosis. As a mechanism for regulatory volume decrease, aquaporins are internalized upon hypotonic stimulation of renal cells [23]. A similar mechanism was also described for lung epithelial cells, in which hypotonicity [5] as well as shear stress [1] resulted in an internalization of aquaporin 5. In these studies, the internalization appeared to be associated to $[Ca^{2+}]_c$ increase. Besides aquaporin internalization, TRPV5 and TRPV6 surface expression is also regulated via $[Ca^{2+}]_c$ [51, 52]. Particularly for TRPV5 channels it was shown that endocytosis depends on clathrin [52]. The obvious dual role of $[Ca^{2+}]_c$ in ATII cells to regulate endocytosis as well as exocytosis might be explained by Minimum model of vesicle processing as proposed by [3]. This model takes into account the duration as well as the intensity of the Ca^{2+} signal and argues that, for slow secretory cell as ATII cells both factors are equally im-

portant for a successful exocytotic event to take place. Furthermore, another finding determined that surfactant exocytosis in these cells can be initiated above a certain threshold of intracellular free Ca^{2+} [18]. Thus, we believe that 2-APB/CPZ stimulation resulted in $[Ca^{2+}]_c$ elevation above the threshold necessary for inducing endocytosis in these cells but the stimulation was still too modest to cause any detectable exocytosis in ATII cells.

The association of 2-APB/CPZ induced Ca^{2+} influx and induction of clathrin dependent endocytosis was clearly demonstrated in our study. However, based on our results, this so far unappreciated effect of 2-APB/CPZ action still remains to be elucidated with regard to binding sites and molecular mechanisms involved. We also demonstrated for the first time that in ATII cells elevation in $[Ca^{2+}]_c$ not only triggers exocytosis but also an opposing endocytotic mechanism.

The observed pharmacological properties of 2-APB/CPZ activated $[Ca^{2+}]_c$ increase fits only partially to known properties of TRP and SOC channels. The fact that these compounds are able to initiate a complex Ca^{2+} influx mechanism, which regulates endocytotic pathway, places them into focus of interest as a new pharmacological tool to investigate clathrin dependent endocytosis.

Acknowledgements

We want to thank Prof. Dr. Paul Walther, Central Electron Microscopy Unit, University of Ulm for helping us with semi-thin slices. The project was supported by the DFG (D1402), the FWF (P15743), the 6th framework of the European Union (Pulmo-Net) and Boehringer Ingelheim.

References

1 Sidhaye VK, Schweitzer KS, Caterina MJ, Shimoda L, King LS: Shear stress regulates aquaporin-5 and airway epithelial barrier function. Proc Nat Acad Sci USA 2008;105:3345-3350.

2 Frick M, Bertocchi C, Jennings P, Haller T, Mair N, Singer W, Pfaller W, Ritsch-Marte M, Dietl P: Ca^{2+} entry is essential for cell strain-induced lamellar body fusion in isolated rat type II pneumocytes. Am J Physiol Lung Cell Mol Physiol 2004;286:L210-L220.

3 Frick M, Eschertzhuber S, Haller T, Mair N, Dietl P: Secretion in Alveolar Type II Cells at the Interface of Constitutive and Regulated Exocytosis. Am J Respir Cell Mol Biol 2001;25:306-315.

4 Ramsey IS, Delling M, Clapham DE: AN INTRODUCTION TO TRP CHANNELS. Annual Review of Physiology 2006;68:619-647.

5 Sidhaye VK, Güler AD, Schweitzer KS, D'Alessio F, Caterina MJ, King LS: Transient receptor potential vanilloid 4 regulates aquaporin-5 abundance under hypotonic conditions. Proc Nat Acad Sci USA 2006;103:4747-4752.

6 Oh-hora M, Yamashita M, Hogan PG, Sharma S, Lamperti E, Chung W, Prakriya M, Feske S, Rao A: Dual functions for the endoplasmic reticulum calcium sensors STIM1 and STIM2 in T cell activation and tolerance. Nat Immunol 2008;9:432-443.

7 Mercer JC, DeHaven WI, Smyth JT, Wedel B, Boyles RR, Bird GS, Putney JW, Jr.: Large Store-operated Calcium Selective Currents Due to Co-expression of Orai1 or Orai2 with the Intracellular Calcium Sensor, Stim1. J Biol Chem 2006;281:24979-24990.

8 Soboloff J, Spassova MA, Tang XD, Hewavitharana T, Xu W, Gill DL: Orai1 and STIM Reconstitute Store-operated Calcium Channel Function. J Biol Chem 2006;281:20661-20665.

9 Vig M, Peinelt C, Beck A, Koomoa DL, Rabah D, Koblan-Huberson M, Kraft S, Turner H, Fleig A, Penner R, Kinet JP: CRACM1 is a plasma membrane protein essential for store-operated Ca^{2+} entry. Science 2006;312:1220-1223.

10 Lis A, Peinelt C, Beck A, Parvez S, Monteilh-Zoller M, Fleig A, Penner R: CRACM1, CRACM2, and CRACM3 are store-operated Ca^{2+} channels with distinct functional properties. Curr Biol 2007;17:794-800.

11 Philipp S, Trost C, Warnat J, Rautmann J, Himmerkus N, Schroth G, Kretz O, Nastainczyk W, Cavalie A, Hoth M, Flockerzi V: TRP4 (CCE1) Protein Is Part of Native Calcium Release-activated Ca^{2+}-like Channels in Adrenal Cells. J Biol Chem 2000;275:23965-23972.

12 Zhu X, Jiang M, Peyton M, Boulay G, Hurst R, Stefani E, Birnbaumer L: trp, a novel mammalian gene family essential for agonist-activated capacitative Ca^{2+} entry. Cell 1996;85:661-671.

13 Singh BB, Liu X, Tang J, Zhu MX, Ambudkar IS: Calmodulin regulates Ca^{2+}-dependent feedback inhibition of store-operated Ca^{2+} influx by interaction with a site in the C terminus of TrpC1. Mol Cell 2002;9:739-750.

14 Liu X, Wang W, Singh BB, Lockwich T, Jadlowiec J, O' Connell B, Wellner R, Zhu MX, Ambudkar IS: Trp1, a Candidate Protein for the Store-operated Ca^{2+} Influx Mechanism in Salivary Gland Cells. J Biol Chem 2000;275:3403-3411.

15 Ong HL, Cheng KT, Liu X, Bandyopadhyay BC, Paria BC, Soboloff J, Pani B, Gwack Y, Srikanth S, Singh BB, Gill D, Ambudkar IS: Dynamic Assembly of TRPC1-STIM1-Orai1 Ternary Complex Is Involved in Store-operated Calcium Influx: Evidence for similarities in store-operated and calcium release-activated calcium channel components. J Biol Chem 2007;282:9105-9116.

16 Ramminger SJ, Richard K, Inglis SK, Land SC, Olver RE, Wilson SM: A regulated apical Na^+ conductance in dexamethasone-treated H441 airway epithelial cells. Am J Physiol Lung Cell Mol Physiol 2004;287:L411-L419.

17 O'Brodovich H, Yang P, Gandhi S, Otulakowski G: Amiloride-insensitive Na^+ and fluid absorption in the mammalian distal lung. Am J Physiol Lung Cell Mol Physiol 2008;294:L401-L408.

18 Haller T, Auktor K, Frick M, Mair N, Dietl P: Threshold calcium levels for lamellar body exocytosis in type II pneumocytes. Am J Physiol Lung Cell Mol Physiol 1999;277:L893-L900.

19 Wemhoner A, Frick M, Dietl P, Jennings P, Haller T: A Fluorescent Microplate Assay for Exocytosis in Alveolar Type II Cells. J Biomol Screen 2006;11:286-295.

20 Dobbs LG, Gonzalez RF, Williams MC: An improved method for isolating type II cells in high yield and purity. Am Rev Respir Dis 1986;134:141-145

21 Bevan S, Hothi S, Hughes GF, James IF, Rang HP, Shah KF, Walpole CS, Yeats JC: Capsazepine: a competitive antagonist of the sensory neurone excitant capsaicin. Br J Pharmacol 1992;107:544-552.

22 Frick MF, Siber GF, Haller TF, Mair NF, Dietl P: Inhibition of ATP-induced surfactant exocytosis by dihydropyridine (DHP) derivatives: a non-stereospecific, photoactivated effect and independent of L-type Ca^{2+} channels. Biochem Pharmacol 2001;61:1161-1167.
23 Tamma G, Procino G, Strafino A, Bononi E, Meyer G, Paulmichl M, Formoso V, Svelto M, Valenti G: Hypotonicity Induces Aquaporin-2 Internalization and Cytosol-to-Membrane Translocation of ICln in Renal Cells. Endocrinology 2007;148:1118-1130.
24 Procino G, Carmosino M, Tamma G, Gouraud S, Laera A, Riccardi D, Svelto M, Valenti G: Extracellular calcium antagonizes forskolin-induced aquaporin 2 trafficking in collecting duct cells. Kidney Int 2004;66:2245-2255.
25 Liu X, Bandyopadhyay B, Nakamoto T, Singh B, Liedtke W, Melvin JE, Ambudkar I: A Role for AQP5 in Activation of TRPV4 by Hypotonicity: concerted involvement of AQP5 and TRPV4 in regulation of cell volume recovery. J Biol Chem 2006;281:15485-15495.
26 Cochilla AJ, Angleson JK, Betz WJ: Monitoring secretory membrane with FM1-43 fluorescence. Annual Review of Neuroscience 1999;22:1-10.
27 Hertel C, Coulter SJ, Perkins JP: A comparison of catecholamine-induced internalization of beta- adrenergic receptors and receptor-mediated endocytosis of epidermal growth factor in human astrocytoma cells. Inhibition by phenylarsine oxide. J Biol Chem 1985;260:12547-12553.
28 Takano M, Koyama Y, Nishikawa H, Murakami T, Yumoto R: Segment-selective absorption of lysozyme in the intestine. Eur J Pharmacol 2004;502:149-155.
29 Visser CC, Stevanovic S, Heleen VL, Gaillard PJ, Crommelin DJ, Danhof M, De Boer AG: Validation of the transferrin receptor for drug targeting to brain capillary endothelial cells in vitro. J Drug Target 2004;12:145-150.
30 Rothberg KG, Ying YS, Kamen BA, Anderson RG: Cholesterol controls the clustering of the glycophospholipid-anchored membrane receptor for 5-methyltetrahydrofolate. J Cell Biol 1990;111:2931-2938.
31 Schnitzer JE, Oh P, Pinney E, Allard J: Filipin-sensitive caveolae-mediated transport in endothelium: reduced transcytosis, scavenger endocytosis, and capillary permeability of select macromolecules. J Cell Biol 1994;127:1217-1232.
32 Smart EJ, Estes K, Anderson RG: Inhibitors that block both the internalization of caveolae and the return of plasmalemmal vesicles. Cold Spring Harb Symp Quant Biol 1995;60:243-8.:243-248.
33 Haller T, Dietl P, Pfaller K, Frick M, Mair N, Paulmichl M, Hess MW, Furst J, Maly K: Fusion pore expansion is a slow, discontinuous, and Ca^{2+}-dependent process regulating secretion from alveolar type II cells. J Cell Biol 2001;155:279-290.
34 Maruyama T, Kanaji T, Nakade S, Kanno T, Mikoshiba K: 2APB, 2-Aminoethoxydiphenyl Borate, a Membrane-Penetrable Modulator of Ins(1,4,5)P3-Induced Ca^{2+} Release. J Biochem 1997;122:498-505.
35 Broad LM, Braun FJ, Lievremont JP, Bird GS, Kurosaki T, Putney JW, Jr.: Role of the Phospholipase C-Inositol 1,4,5-Trisphosphate Pathway in Calcium Release-activated Calcium Current and Capacitative Calcium Entry. J Biol Chem 2001;276:15945-15952.
36 Prakriya M, Lewis RS: Potentiation and inhibition of Ca^{2+} release-activated Ca^{2+} channels by 2-aminoethyldiphenyl borate (2-APB) occurs independently of IP3 receptors. J Physiol 2001;536:3-19.
37 Braun FJ, Aziz O, Putney JW, Jr.: 2-Aminoethoxydiphenyl Borane Activates a Novel Calcium-Permeable Cation Channel. Mol Pharmacol 2003;63:1304-1311.
38 Feske S, Gwack Y, Prakriya M, Srikanth S, Puppel SH, Tanasa B, Hogan PG, Lewis RS, Daly M, Rao A: A mutation in Orai1 causes immune deficiency by abrogating CRAC channel function. Nature 2006;441:179-185.
39 DeHaven WI, Smyth JT, Boyles RR, Bird GS, Putney JW, Jr.: Complex Actions of 2-Aminoethyldiphenyl Borate on Store-operated Calcium Entry. J Biol Chem 2008;283:19265-19273.
40 Hu HZ, Gu Q, Wang C, Colton CK, Tang J, Kinoshita-Kawada M, Lee LY, Wood JD, Zhu MX: 2-Aminoethoxydiphenyl Borate Is a Common Activator of TRPV1, TRPV2, and TRPV3. J Biol Chem 2004;279:35741-35748.
41 Flemming RF, Xu SZ, Beech DJ: Pharmacological profile of store-operated channels in cerebral arteriolar smooth muscle cells. Br J Pharmacol 2003;139:955-965.
42 Jiang NF, Zhang ZM, Liu L, Zhang C, Zhang YL, Zhang ZC: Effects of Ca^{2+} channel blockers on store-operated Ca^{2+} channel currents of Kupffer cells after hepatic ischemia/reperfusion injury in rats. World J Gastroenterol 2006;12:4694-4698.
43 Clapham DE, Julius D, Montell C, Schultz G: International Union of Pharmacology. XLIX. Nomenclature and Structure-Function Relationships of Transient Receptor Potential Channels. Pharmacol Rev 2005;57:427-450.
44 Gunthorpe MJ, Rami HK, Jerman JC, Smart D, Gill CH, Soffin EM, Luis Hannan S, Lappin SC, Egerton J, Smith GD, Worby A, Howett L, Owen D, Nasir S, Davies CH, Thompson M, Wyman PA, Randall AD, Davis JB: Identification and characterisation of SB-366791, a potent and selective vanilloid receptor (VR1/TRPV1) antagonist. Neuropharmacology 2004;46:133-149
45 Gavva NR, Tamir R, Qu Y, Klionsky L, Zhang TJ, Immke D, Wang J, Zhu D, Vanderah TW, Porreca F, Doherty EM, Norman MH, Wild KD, Bannon AW, Louis JC, Treanor JJ: AMG 9810 [(E)-3-(4-t-butylphenyl)-N-(2,3-dihydrobenzo[b][1,4] dioxin-6-yl)acrylamide], a novel vanilloid receptor 1 (TRPV1) antagonist with antihyperalgesic properties. J Pharmacol Exp Ther 2005;313:474-484.
46 Bayer N, Schober D, Prchla E, Murphy RF, Blaas D, Fuchs R: Effect of Bafilomycin A1 and Nocodazole on Endocytic Transport in HeLa Cells: Implications for Viral Uncoating and Infection. J Virol 1998;72:9645-9655.
47 Wissel H, Lehfeldt A, Klein P, Muller T, Stevens PA: Endocytosed SP-A and surfactant lipids are sorted to different organelles in rat type II pneumocytes. Am J Physiol Lung Cell Mol Physiol 2001;281:L345-L360.
48 Ruckert P, Bates SR, Fisher AB: Role of clathrin- and actin-dependent endocytotic pathways in lung phospholipid uptake. Am J Physiol Lung Cell Mol Physiol 2003;284:L981-L989.
49 Chen Y, Deng L, Maeno-Hikichi Y, Lai M, Chang S, Chen G, Zhang JF: Formation of an endophilin-Ca^{2+} channel complex is critical for clathrin-mediated synaptic vesicle endocytosis. Cell 2003;115:37-48.
50 Musch MW, Arvans DL, Walsh-Reitz MM, Uchiyama K, Fukuda M, Chang EB: Synaptotagmin I binds intestinal epithelial NHE3 and mediates cAMP- and Ca^{2+}-induced endocytosis by recruitment of AP2 and clathrin. Am J Physiol Gastrointest Liver Physiol 2007;292:G1549-G1558.
51 van de Graaf SFJ, Chang Q, Mensenkamp AR, Hoenderop JGJ, Bindels RJM: Direct Interaction with Rab11a Targets the Epithelial Ca^{2+} Channels TRPV5 and TRPV6 to the Plasma Membrane. Mol Cell Biol 2006;26:303-312.
52 van de Graaf SFJ, Rescher U, Hoenderop JGJ, Verkaart S, Bindels RJM, Gerke V: TRPV5 Is Internalized via Clathrin-dependent Endocytosis to Enter a Ca^{2+}-controlled Recycling Pathway. J Biol Chem 2008;283:4077-4086.